Conference Paper, Published Version

Lopez-Caballero, Fernando; Modaressi-Farahmand-Razavi, A.

Mitigation of liquefaction seismic risk by preloading

ISGSR 2011 - Vogt, Schuppener, Straub & Bräu (eds) - © 2011 Bundesanstalt für Wasserbau ISBN 978-3-939230-01-4

Mitigation of liquefaction seismic risk by preloading

F. Lopez-Caballero & A. Modaressi-Farahmand-Razavi
Laboratoire MSS-Mat CNRS UMR 8579, Ecole Centrale Paris, Châtenay-Malabry, France

ABSTRACT: The present paper deals with the use of numerical methods so as to assess the efficiency of an improvement method to reduce the liquefaction potential in a sandy soil profile subjected to shaking. The objective is to reveal the beneficial or unfavorable effects of preloading method on the soil response. This analysis shows the efficiency of the preloading in the mitigation of a liquefiable soil but the intervention at the foundation soil modifies the dynamic characteristics of the signal at surface.

Keywords: Liquefaction, Mitigation Methods, Numerical simulation

1 INTRODUCTION

In practice, in order to mitigate the damage effects of earthquake induced liquefaction in engineering structures, the countermeasure methods such as gravel drains, soil densification or confinement walls among others are used. Such methods are studied by several authors and the principal conclusion of these works is that the efficiency of each solution depends on many parameters (e.g. input signal characteristic, soil properties).

The aim of this work is to assess numerically the efficiency of the soil densification using preloading techniques on the improvement of liquefiable sandy profiles to shaking. Preloading is a temporary loading, usually an embankment, applied at a construction site to improve subsurface soils by densification and increase in lateral stress. For construction sites where sandy layers are predominant, experience has illustrated that about three weeks suffice for soil improvement to take place. The method is frequently used to improve bad soil conditions and make them sustain large static loads (Stamatopoulos and Kotzias, 1985; Petridis et al., 2000).

A finite element modelling is carried out in order to study the influence of the input motion on both the response of the soil profile and the possibility that liquefaction phenomena appear. An elastoplastic multimechanism model is used to represent the soil behaviour. A numerical probabilistic analysis is performed so as to quantify the impact of the uncertainties associated with the input signal and the mitigation method on both the ground motion at the surface and the apparition of liquefaction phenomena. Thus, a liquefaction reliability index profile can be obtained for the profile with or without mitigation for a given seismic hazard.

2 NUMERICAL MODEL

A typical layered soil/rock model is considered. The soil profile is composed principally of clay layers overlaid by 22m of loose sand (i.e. a relative density Dr < 50%). The total thickness of the soil profile is 40m over the bedrock. The numerical model is based on the site measurement of SPT-N_{60} and shear wave velocities (Vs) given in Figure 1 (Lopez-Caballero and Modaressi-Farahmand-Razavi, 2008). The fundamental elastic period of the soil profile is 0.57s. According to the SPT test results and the soil description, it is deduced that the liquefaction phenomena can appear at layers between 4m and 15m depth (SPT-N_{60} between 4 and 10) as from 22m depth the soil is composed principally of overconsolidated clay.

Thus, an elastoplastic model is only used to represent the soil behaviour on the top 29m. In these layers, the shear modulus of the soil increases with depth. For the soil between 29m and 40m, isotropic linear elastic soil behaviour is assumed. The deformable bedrock is placed at 40m depth.

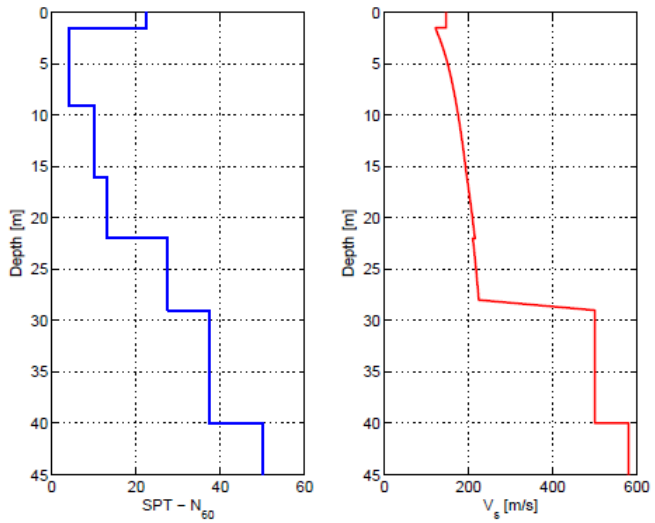

Figure 1. SPT and S velocity profiles of the site and adopted in the numerical analysis.

2D u-p_w coupled finite elements computations with plane-strain assumption are performed. The saturated soil was modelled using quadrilateral isoparametric elements with eight nodes for both solid displacements and fluid pressures. The thickness of the plane-strain elements is 0.5m. An implicit Newmark numerical integration scheme with γ=0.625 and β=0.375 is used in the dynamic analysis (Katona and Zienkiewicz, 1985).

In order to investigate the effect of the preloading method on the response of the soil profile, a comparative dynamical response analysis at the end of shaking for the cases with and without mitigation method is done.

2.1 *Boundary conditions*

In the analysis, only vertically incident shear waves are introduced into the domain and as the response of an infinite semi-space is modelled, equivalent boundaries have been imposed on the nodes of lateral boundaries (i.e. the normal stress on these boundaries remains constant and the displacements of nodes at the same depth in two opposite lateral boundaries are the same in all directions). For the bedrock's boundary condition, paraxial elements simulating“deformable unbounded elastic bedrock” have been used (Modaressi and Benzenati, 1994). The incident waves, defined at the outcropping bedrock are introduced into the base of the model after deconvolution. Thus, the obtained movement at the bedrock is composed of the incident waves and the reflected signal. The bedrock is supposed to be impervious and the water level is placed at the ground surface.

2.2 *Soil model*

The elastoplastic multi-mechanism model developed at Ecole Centrale Paris, known as ECP model (Aubry et al. 1982; Hujeux, 1985) is used to represent the soil behaviour. This model can take into account the soil behaviour in a large range of deformations. The model is written in terms of effective stress. The representation of all irreversible phenomena is made by four coupled elementary plastic mechanisms: three plane-strain deviatoric plastic deformation mechanisms in three orthogonal planes and an isotropic one. The model uses a Coulomb-type failure criterion and the critical state concept. The evolution of hardening is based on the plastic strain (deviatoric and volumetric strain for the deviatoric mechanisms and volumetric strain for the isotropic one). To take into account the cyclic behaviour a kinematical hardening based on the state variables at the last load reversal is used. The soil behaviour is decomposed into pseudo-elastic, hysteretic and mobilized domains. Refer to (Aubry et al. 1982; Hujeux 1985; Lopez-Caballero and Modaressi-Farahmand-Razavi, 2008) among others for further details about the ECP model. For sake of brevity only some models' definitions are given in what follows. Adopting the soil

mechanics sign convention (compression positive), the deviatoric primary yield surface of the *k* plane is given by:

$$f_k = q_k - \sin\phi'_{pp} \cdot p'_k \cdot F_k \cdot r_k \qquad (1)$$

Where, p'_k and q_k are the mean and deviatoric values of stress tensors, ϕ'_{pp} is the friction angle at the critical state, the function F_k permits to control the isotropic hardening associated with the plastic volumetric strain, whereas r_k accounts for the isotropic hardening generated by plastic shearing. They represent progressive friction mobilization in the soil and their product reaches unity at perfect plasticity. Therefore, in order to provide for any state a direct measure of "distance to reach the critical state" (r_k) and based upon our elastoplastic model, it is possible to define an apparent friction angle (ϕ'_{apt}) by:

$$\sin\phi'_{apt} = \frac{q_k}{p'_k \cdot F_k} \qquad (2)$$

$$r_k = \frac{\sin\phi'_{apt}}{\sin\phi'_{pp}} \qquad (3)$$

2.3 *Input earthquake motion*

In order to define appropriate input motions to the non-linear coupled dynamical analysis, a selection of recorded accelerograms is used. The adopted earthquake signals are proposed by (Iervolino and Cornell, 2005; Sorrentino et al. 2008). Thus, 142 unscaled records were chosen from the Pacific Earthquake Engineering Research Center (PEER) database. The events range in magnitude between 5.2 and 7.6 and the recordings are at site-to-source distances from 15 to 50km and dense-to-firm soil conditions (i.e. 360m/s < $V_{s\ 30m}$ < 800m/s).

Concerning the response spectra of input earthquake motions, Figure 2 shows the mean and the response spectra curves with a probability of exceedance (PE) between 2.75 and 97.5%. It can be noted that the mean response spectra is consistent with the response spectra of Type A soil of Eurocode8 scaled to the mean outcropping a_{max} value. The uncertainty on some input earthquake characteristics obtained for the strong ground motions are summarized in Table 1. These earthquake characteristics are maximal outcropping acceleration (a_{max}), Arias intensity (I_{Arias}), predominant period (Tp), mean period (Tm), period of equivalent harmonic wave ($T_{V/A}$=α pgv/pga), spectral intensity (SI), peak ground velocity (pgv), root-mean-square intensity (I_{rms}), Cosenza and Manfredi dimensionless index (I_D) and the significant duration ($t_{5\ 95}$).

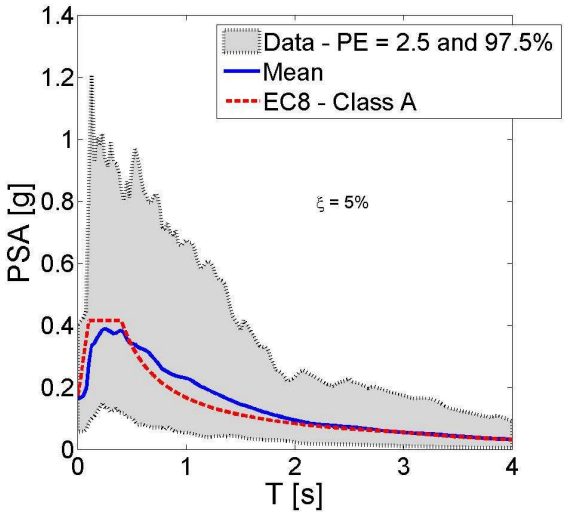

Figure 2. Response spectra of input earthquake motions

Table 1. Uncertain earthquake characteristics for the selected earthquakes

Parameter	Range	Mean	CV [%]
a_{max} [g]	0.04-0.60	0.17	56
Tm [s]	0.28-1.46	0.66	34
Tp [s]	0.10-1.10	0.37	58
$T_{V/A}$ [s]	0.23-1.43	0.58	38
I_{Arias} [m/s]	0.03-5.90	0.59	131
$t_{5\,95}$ [s]	4.40-51.4	19.0	44
I_{rms} [m/s^2]	0.10-1.21	0.26	55
pgv [m/s]	0.03-0.62	0.19	58
I_D [.]	2.97-27.3	10.5	45
SI [m]	0.12-2.52	0.70	57

2.4 *Preloading simulation*

In order to simulate the construction and demolition of the preload embankment, the calculations are performed in two steps. In the first step, since soil behaviour is a function of the effective stress state for nonlinear elastoplastic models, initial in-situ stress state due to gravity loads are computed. After this initialization, the displacements and deformations are eliminated and the initial effective stresses, pore-water pressures and model history variables are stored to be used as initial state of the second step computation. In the second one, a sequential level-by-level construction and demolition of the embankment is performed.

The embankment load is applied as a prescribed normal stress time history at the surface of soil profile. In order to assess the effect of static load applied on the response of the soil profile, two embankment heights were studied, 4 and 8m with a density equal to 2400kg/m^3. The embankment is constructed and demolished in 18.5 days and it stays in place during 3 months before the application of the seismic event. After this period, all over pore pressures are dissipated.

3 LIQUEFACTION ANALYSIS

In order to define the liquefaction reference case, the responses obtained by the model without preloading are analysed. It can be noted from the pore pressure excess (Δp_w) in the soil profile obtained at the end of the signal (i.e. coseismic analyses) for all simulations (Figure 3), that regarding the mean response obtained, the liquefaction phenomenon does not occur (i.e. $\Delta p_w < \sigma'_{vo}$). Otherwise, concerning all simulations, in some cases the apparition of liquefaction is found at layers between 2 and 15m depth. Assuming that the liquefaction appears when the pore pressure ratio ($r_u=\Delta p_w/\sigma'_{vo}$) is greater than 0.8, a liquefaction probability profile could be estimated. The liquefaction probability is estimated as $p_f(z)=N_f(z)/N$, where $N_f(z)$ is the number of simulations when $r_u \geq 0.8$ at depth z and N is the total number of simulations. Using this approach, a profile of Prob[$r_u \geq 0.8$] as a function of depth is presented in Figure 4. According to these results, the maximum liquefaction probability is 32% between 4 and 6m deep.

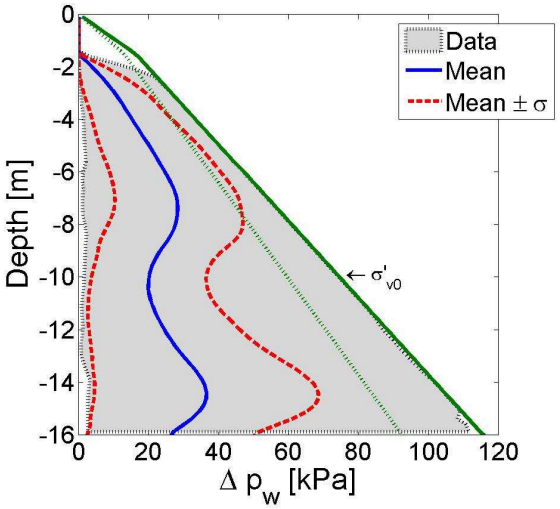

Figure 3. Obtained pore pressure excess in the soil profile

So as to quantify the effect of the liquefaction phenomena, we use the computed Liquefaction Index (Q) for the profile. This parameter is defined by Shinozuka and Ohtomo (1989) as:

$$Q = \frac{1}{H}\int_0^H \frac{\Delta p_w(t,z)}{\sigma'_{vo}(z)}\,dz \qquad (4)$$

where H is the selected depth (in this case, H=10m), $\Delta p_w(t, z)$ is the pore water pressure build-up computed at time t and depth z and $\sigma'_{vo}(z)$ is the initial effective vertical stress at depth z. Figure 5 provides the variation of Q value at the end of shaking with maximum acceleration at the outcropping bedrock ($a_{max\ out}$). Referring again to Figure 5, it can be seen that as expected, the $Q_{H=10m}$ value increases with an increase in $a_{max\ out}$ value. It appears that $a_{max\ out}$ value provides a good correlation with the thickness of the zones where liquefaction takes place (i.e. the liquefaction index).

In order to study the effect of the random shaking on the amplitude of the acceleration obtained at the surface level, Figure 6 shows the variation of peak ground acceleration at the surface (pga) as a function of the maximum acceleration at the outcropping bedrock ($a_{max\ out}$). According to this figure, the amplification of peak ground acceleration on the ground surface relative to bedrock appears before $a_{max\ out}$ value equal to 0.12g.

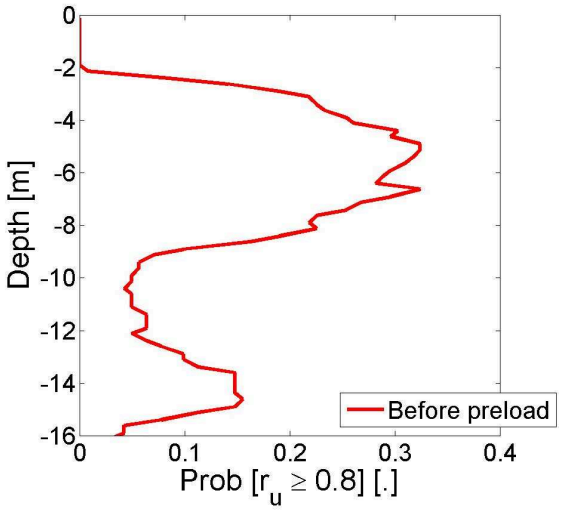

Figure 4. Evolution of liquefaction probability with depth. Case before preloading.

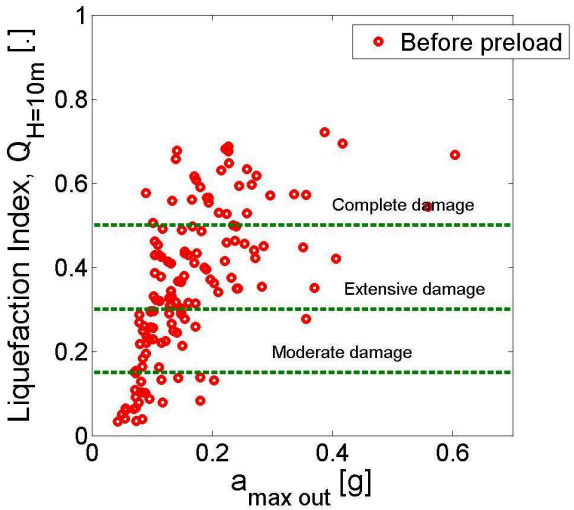

Figure 5. Scatter plot of obtained $Q_{H=10m}$ values as a function of $a_{max\ out}$. Case before preloading.

4 ANALYSIS OF LIQUEFACTION IMPROVEMENT METHOD

In this section, a mitigation method (i.e. preloading) is used in order to improve the ground and to prevent liquefaction apparition. The selected mitigation method reduces the liquefaction potential stiffening the soil and then decreases the settlement. Figure 7 provides a comparison of the mean pore pressure excess

(Δp_w) profile at the end of shaking for the case before preloading and after the two preloading cases (i.e. two embankment heights). A comparison of distribution of Δp_w profiles indicates that, the pore pressure build up decreases strongly when the preloading is used. The comparison between the profile of r_k value (equation 3) before and after the two preloading cases (Figure 8) shows that after the loading and unloading due to mitigation method the "distance to reach the critical state" increases. It produces a soil stiffening effect that allows a reduction of the pore pressure excess.

It is also observed that according to Figure 9, the maximum liquefaction probability decreases from 32% in the reference case to 20%, when the 8m high embankment is considered.

As already mentioned, the remediation method used increases the liquefaction strength and in consequence it will decrease the soil settlement. However, regarding the variation of *pga* values at the surface (Figure 10), it appears that in some cases, it increases because of the soil stiffening effect, hence it could be an unfavorable method from the structural viewpoint.

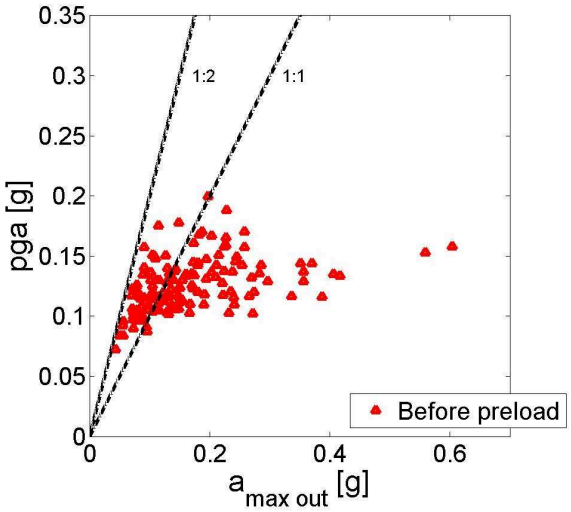

Figure 6. Relationships between maximum outcropping accelerations $a_{max\ out}$ and surface pga obtained for different earthquakes.

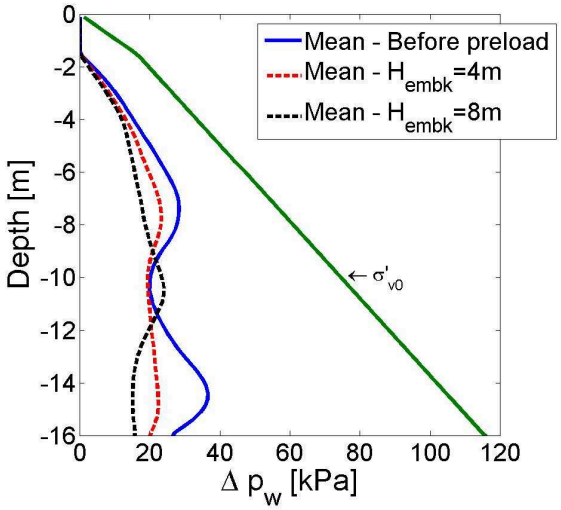

Figure 7. Effect of embankment height on the obtained pore pressure excess in the soil profile.

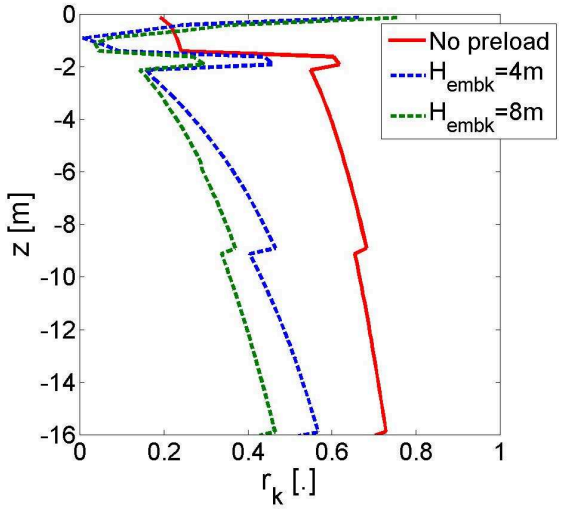

Figure 8. Effect of embankment height on the obtained r_k parameter in the soil profile.

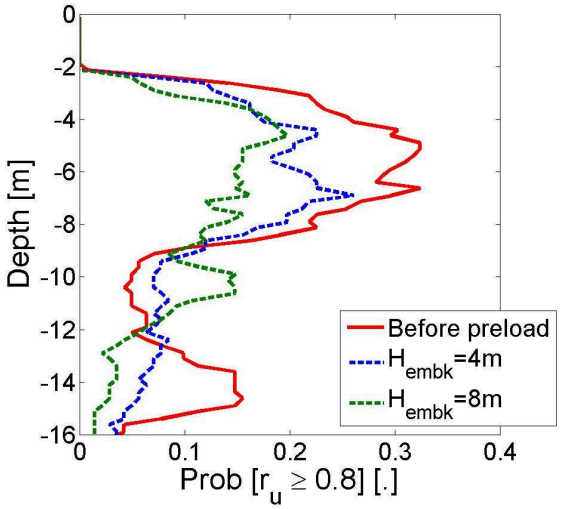

Figure 9. Effect of embankment height on the evolution of liquefaction probability with depth.

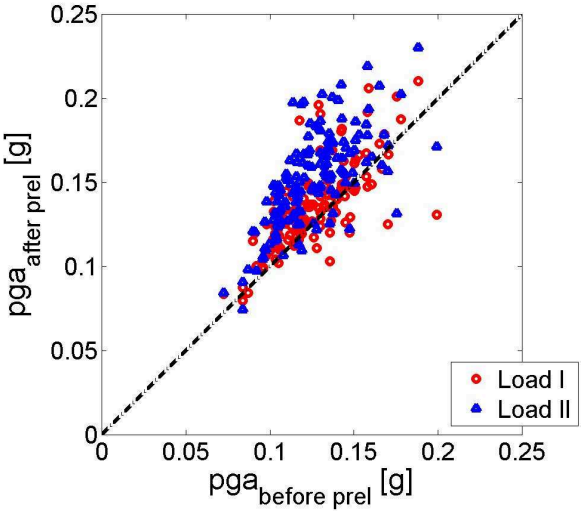

Figure 10. Scatter plot of variation of pga values before and after preloading.

5 VULNERABILITY ANALYSIS

Finally, three damage levels are chosen and showed in Figure 5. They correspond to a moderate liquefaction (Q_{lim} = 0.15), extensive liquefaction (Q_{lim} = 0.3) and complete liquefaction (Q_{lim} = 0.5). Figure 11

presents fitted fragility functions obtained for the second damage level (i.e. extensive damage) with respect to $a_{max\ out}$ for the three studied cases (i.e. before and after preloading). If the fragility curves obtained before and after preloading are compared, it is observed that for all values of $a_{max\ out}$, higher probability to exceed the Q_{lim} value is found before mitigating the soil. A similar behaviour is found for the others Q_{lim} values.

6 CONCLUSIONS

A series of finite element parametric analyses were performed to investigate the effects of the liquefaction countermeasures on the behaviour of soil profile. The main conclusions drawn from this study are as follows.

According to the responses obtained with the model without mitigation, it can be concluded that the choice of the "bedrock" signal remains the most subtle parameter in order to define the liquefiable zones and the characteristics of possible countermeasures. Thus, a parametric analysis is needed in order to study the influence of several signal parameters on the response of the site soil profile.

The analyses showed that the use of the preloading reduces the excess pore pressure generation into the soil profile. As a consequence, for a given seismic hazard the liquefaction probability decreases when the mitigation method is used. However, it increases the amplitude of the surface ground motion which could be a disadvantage on a structural viewpoint.

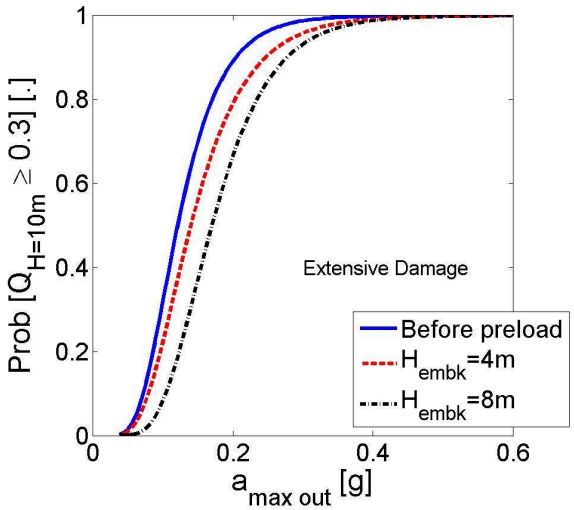

Figure 11. Fragility curves for extensive damage level as a function of $a_{max\ out}$. Effect of mitigation method.

ACKNOWLEDGEMENTS

This study has been done in the framework of the European Community Contract No FP7-SME-2010-1-262161-PREMISERI (PREloading to MItigate SEismic RIsk).

REFERENCES

Aubry, D., Hujeux J.-C.,Lassoudière F., & Meimon Y. 1982. A double memory model with multiple mechanisms for cyclic soil behaviour. In Int. Symp. Num. Mod. Geomech, pp. 3–13. Balkema.

Hujeux, J.-C. 1985. Une loi de comportement pour le chargement cyclique des sols. In Génie Parasismique, pp. 278–302. V. Davidovici, Presses ENPC, France.

Iervolino, I. & Cornell, C. A. 2005. Record selection for nonlinear seismic analysis of structures, Earthquake Spectra 21(3), 685–713.

Katona, M. G. & O. C. Zienkiewicz 1985. A unified set of single step algorithms part 3: the beta-mmethod, a generalization of the newmark scheme. International Journal of NumericalMethods in Engineering 21(7), 1345–1359.

Lopez-Caballero, F. & Modaressi-Farahmand-Razavi A. 2008. Numerical simulation of liquefaction effects on seismic SSI. Soil Dynamics and Earthquake Engineering 28(2), 85–98.

Modaressi, H. & Benzenati I. 1994. Paraxial approximation for poroelastic media. Soil Dynamics and Earthquake Engineering 13(2), 117–129.

Petridis P., Stamatopoulos C. & Stamatopoulos A. (2000). Soil Improvement by preloading of two erratic sites. GeoEng2000, International conference on Geotechnical and Geological Engineering, Melbourne, Australia (on CD, 7 pages).
Shinozuka, M. & Ohtomo K. 1989. Spatial severity of liquefaction. In Proceedings of the second US-Japan workshop in liquefaction, Large Ground Deformation and Their Effects on Lifelines.
Sorrentino, L., Kunnath S., Monti G., & Scalora G. 2008. Seismically induced one-sided rocking response of unreinforced masonry façades. Engineering Structures 30(8), 2140–2153.
Stamatopoulos A. C., & Kotzias P. C. (1985). Soil Improvement by Preloading, John Wiley & Sons, 261 pages, 1985.